

13. Reid, P. A. & Watts, C. Cycling of cell-surface MHC glycoproteins through primaquine-sensitive intracellular compartments. *Nature* **346**, 655–657 (1990).
14. Neefjes, J. J., Stollorz, V., Peters, P. J., Geuze, H. J. & Ploegh, H. L. The biosynthetic pathway of MHC class II but not class I molecules intersects the endocytic route. *Cell* **61**, 171–183 (1990).
15. Roosnek, E., Demotz, S., Corradin, G. & Lanzavecchia, A. Kinetics of MHC–antigen complex formation on antigen-presenting cells. *Immunol.* **140**, 4079–4082 (1988).
16. Lanzavecchia, A., Reid, P. A. & Watts, C. Irreversible association of peptides with class II MHC molecules in living cells. *Nature* **357**, 249–252 (1992).
17. Nelson, C. A., Petzold, S. J. & Unanue, E. R. Peptides determine the lifespan of MHC class II molecules in the antigen-presenting cell. *Nature* **371**, 250–252 (1994).
18. Amigorena, S., Drake, J. R., Webster, P. & Mellman, I. Transient accumulation of new class II MHC molecules in a novel endocytic compartment in B lymphocytes. *Nature* **369**, 113–120 (1994).
19. Germain, R. N. & Hendrix, L. R. MHC class II structure, occupancy and surface expression determined by post-endoplasmic reticulum antigen binding. *Nature* **353**, 134–139 (1991).
20. Pierre, P. *et al.* Developmental regulation of MHC class II transport in mouse dendritic cells. *Nature* this issue. EDS to complete on page

Acknowledgements. We thank D. Scheidegger and M. Dessing for technical assistance, E. Long for discussion, and C. Watts, F. Sallusto, K. Karjalainen and M. Colonna for critically reading the manuscript. The Basel Institute for Immunology was founded and is supported by F. Hoffmann–La Roche, Basel, Switzerland.

Correspondence and requests for material should be addressed to M.C. (e-mail: cella@bii.ch).

Developmental regulation of MHC class II transport in mouse dendritic cells

Philippe Pierre*, Shannon J. Turley*, Evelina Gatti, Michael Hull, Joseph Meltzer†, Asra Mirza†, Kayo Inaba†, Ralph M. Steinman† & Ira Mellman

Department of Cell Biology, Yale University School of Medicine, 333 Cedar Street, PO Box 208002, New Haven, Connecticut 06520, USA

† The Rockefeller University, 1230 York Avenue, New York, New York 10021, USA

* These authors contributed equally to this work.

Dendritic cells (DCs) have the unique capacity to initiate primary and secondary immune responses^{1–3}. They acquire antigens in peripheral tissues and migrate to lymphoid organs where they present processed peptides to T cells. DCs must therefore exist in distinct functional states, an idea that is supported by observations that they downregulate endocytosis and upregulate surface molecules of the class II major histocompatibility complex (MHC) upon maturation^{4–7}. Here we investigate the features of DC maturation by reconstituting the terminal differentiation of mouse DCs *in vitro* and *in situ*. We find that early DCs, corresponding to those found in peripheral tissues, exhibit a phenotype in which most class II molecules are intracellular and localized to lysosomes. Upon maturation, these cells give rise to a new intermediate phenotype in which intracellular class II molecules are found in peripheral non-lysosomal vesicles, similar to the specialized CIIV population seen in B cells. The intermediate cells then differentiate into late DCs which express almost all of their class II molecules on the plasma membrane. These variations in class II compartmentalization are accompanied by dramatic alterations in the intracellular transport of the new class II molecules and in antigen presentation. We found that although early DCs could not present antigen immediately after uptake, efficient presentation of the previously internalized antigen occurred after maturation, 24–48 hours later. By regulating class II transport and compartmentalization, DCs are able to delay antigen display, a property crucial to their role in immune surveillance.

Mouse bone marrow is a major source of DCs when cultivated with granulocyte–macrophage colony-stimulating factor (GM-CSF)⁸. Immunofluorescence microscopy of these cultures revealed three distinct developmental stages. Cells were identified as DCs by the expected repertoire of antigens and expression of MHC class II, cell shape, and adherence. As reported previously⁸, DCs were found

by immunofluorescence or FACS to be negative or weakly positive for the granulocyte marker GR1, negative for the macrophage marker SER-4, but strongly positive for CD11c and MHC class II. Contaminating SER-4 or GR1-positive cells were negative for class II and judged not to be DCs.

After 4–5 days, DCs were found in proliferating clusters loosely attached to adherent stromal cells⁸. By confocal microscopy, most of the cells present in or migrating out from the clusters showed little MHC class II on their surface, but contained abundant intracellular class II (Fig. 1a). The class II-positive vesicles represented lysosomes (MIICs) and late endosomes, being positive for Ig γ -B/lamp-2 and H2-M (Fig. 1a). Thus, they were characteristic of MIIC as defined in human lymphoblasts and human DCs^{9–12}. As the MIIC-containing cells were present in proliferating clusters, we defined them as ‘early’ DCs.

With increasing time in culture, two additional cell populations were detected. The first of these (‘intermediate’ DCs) was present transiently and comprised non-adherent cells that had little surface MHC class II (Fig. 1b). They were strikingly unlike the early cells, however, because most of their intracellular class II was in a vesicle population that was devoid of lysosomal markers (Fig. 1b, arrows), and thus reminiscent of non-lysosomal, class II-positive CIIV isolated from A20 B cells¹³. At later times in particular, the vesicles accumulated directly beneath the plasma membrane (Fig. 1b, right), whereas the lysosomes became concentrated in the perinuclear region.

The third major DC population accumulated with time until by 8–10 days it represented almost all of the non-adherent class II-positive cells. These ‘late’ cells had a more classical DC phenotype, with long processes that stained for class II (green) (Fig. 1c). Little class II remained intracellularly, with most of the now largely class II-depleted H2-M/lamp-positive lysosomes visualized as poorly resolved clusters of red-staining vesicles in the perinuclear region. Further characterization indicated that markers such as DEC-205 and 2A1 were absent from early cells but expressed at moderate and high levels on intermediate and late cells, respectively^{8,14} (results not shown). Early cells, but not late cells, were capable of efficient fluid endocytosis (W. Garrett and I.M., unpublished results), as found previously for human cells⁴.

To determine whether early cells pass through the intermediate phenotype before reaching maturity, we produced highly purified populations of early cells by gently dislodging and isolating proliferating clusters on serum columns, followed by depletion of contaminating cells by fluorescent-activated cell sorting (FACS)⁸. This approach yielded ~95% pure populations of early DCs. As quantified in Fig. 1d, after 5–8 h in culture, the early cells had nearly disappeared and >60% of the population of exhibited the intermediate phenotype (for example, see Fig. 1b); 20–30% exhibited the late or mature phenotype (as shown in Fig. 1c). After 24 h, ~90% of the cells were found to be of the late phenotype. As the number of cells remained constant throughout, these results strongly suggest that there is a sequential relationship in the maturation pathway. The rapid maturation kinetics observed using purified cluster-derived cells probably reflect their greater developmental synchrony.

To ensure that the developmental sequence was not peculiar to bone marrow cultures, we investigated whether tissue DCs had similar properties. We first examined epidermal Langerhans cells¹⁵. In epidermal explants, class II was present in these cells in a punctuate pattern which co-localized with lysosomal marker H2-M, reminiscent of early bone marrow DCs (Fig. 2, upper right panels). If explants were incubated in culture medium and the Langerhans cells allowed to mature *in situ*, within 4 h the degree of class II and H2-M co-localization decreased, with class II staining remaining punctuate but becoming progressively less coincident with H2-M, which became concentrated at the cell body (Fig. 2, right panels). This pattern was consistent with the intermediate

phenotype. By 8 h, class II staining appeared homogeneous over the entirety of the cell, suggesting that it was present on the plasma membrane (fig. 2, lower right panels), consistent with cells of the late phenotype.

These results were confirmed by monitoring the development of Langerhans cells isolated from the explants¹⁶, which were found to follow the same morphological transitions observed using the bone marrow cultures (Fig. 2, left panels). Similar results were obtained for splenic DCs derived from red pulp (not shown). Thus, DCs in peripheral tissues adopt the early phenotype but can be induced by isolation, cytokine exposure or physical disruption to undergo the same type of maturational pattern as DCs in bone marrow culture.

The shift of MHC class II from lysosomal to non-lysosomal structures was confirmed by immuno-electron microscopy and by cell fractionation in Percoll density gradients; MHC class II $\alpha\beta$ dimers in lysosomal and non-lysosomal fractions alike were found in the SDS-stable conformation, suggesting that they were loaded with peptide (not shown). Of greater interest was to determine

whether the sequential appearance of class II in lysosomal then non-lysosomal structures reflected a shift of intracellular class II from lysosome-like MIIC to endosome-like class II vesicles (CIIV), similar those found in murine B cells¹³. CIIVs represent a distinct vesicle population and are resolved from conventional endocytic organelles by free-flow electrophoresis¹⁷. We fractionated early and late DC populations by free-flow electrophoresis and found, as expected, that each population had a typical fractionation pattern: plasma membrane markers (LFA-1 detected by western blot) were restricted to unshifted fractions containing the major peak of cell proteins, whereas endosome- and lysosome-containing fractions (detected by β -hexosaminidase) were deflected towards the anode (results not shown).

When the free-flow electrophoresis fractions were probed by western blotting (Fig. 3a), early DCs exhibited class II in unshifted fractions (containing endoplasmic reticulum, Golgi and plasma membranes), as well as in fractions that co-migrated with lysosomal markers. The pattern was similar for cultures containing intermedi-

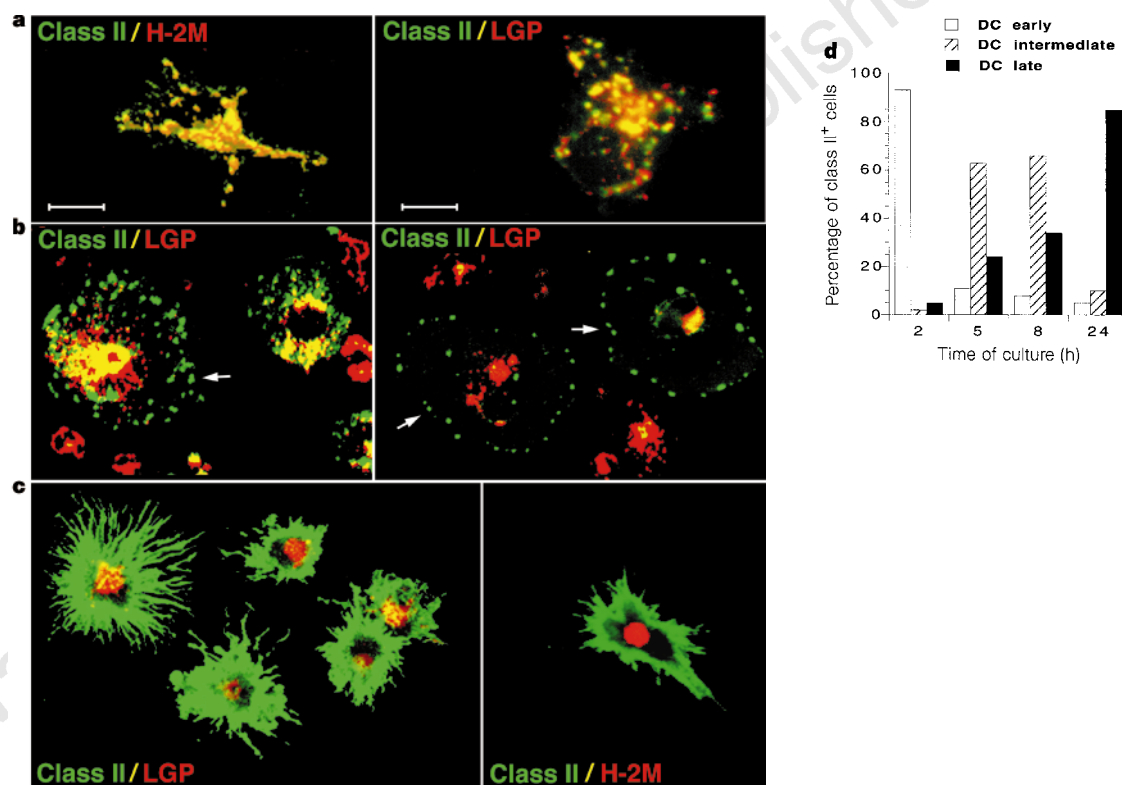


Figure 1 MHC class II distribution defines three distinct stages in the developmental maturation of bone-marrow-derived dendritic cells *in vitro*. DCs from bone marrow cultures were collected, plated on glass coverslips, and processed for immunofluorescence and confocal microscopy. In each case, MHC class II molecules were visualized using an FITC-conjugated second antibody and displayed as green staining. **a**, Early-DC phenotype. Optically merged confocal image of cells derived from proliferating clusters and stained for H2-M (red, left) or lysosomal membrane protein lgp-B/lamp-2 (LGP, red; right) and class II (green). Cells were isolated on day 4 of culture in the presence of GM-CSF. Class II co-localizes with both H2-M and lgp/lamp (yellow). Scale bars, 10 μ m. **b**, Intermediate-DC phenotype. Optically merged confocal image of non-adherent cells stained for lgp-B/lamp-2 (red) and class II (green) after 6–7 days of culture in the presence of GM-CSF. Arrows indicate the presence of class II-containing vesicles depleted of lysosomal markers. Cells in the images on the left in the panels are the first to appear in culture and still contain some co-localized class II and lysosomal markers in the perinuclear region. Cells in the images on the right appear later and show a typical alignment of the non-lysosomal CIIV-like structures just beneath the plasma membrane. The CIIV-like structures were all unlikely to be macropinosomes as they were negative for surface markers MHC class I and LFA-1, both of which gave circumferential staining (not shown). Class II-negative cells staining for lgp/lamp in the field represent granulocyte or monocyte contaminants of the culture. **c**, Late DC phenotype. Optically merged confocal image of non-adherent DC stained for lgp-B/lamp-2 (left, red) or H2-M (right red) and class II (green) on day 8 of culture. All cells have a dendritic, sea-urchin-like appearance, with most class II molecules now on the cell surface. Lysosomes often appeared as a poorly resolved cluster concentrated in the perinuclear cytoplasm and devoid of MHC class II. **d**, Sequential appearance of early, intermediate and late DC phenotypes in highly purified cultures. Proliferating clusters were isolated on 50%-serum columns and early DCs further purified by depletion of GR1-positive granulocyte by FACS. Nearly homogeneous populations of early cells (95% pure) were returned to culture in the presence of GM-CSF and assayed by immunofluorescence microscopy at after 2, 5, 8 and 24 h. The total number of cells was constant at each time point, indicating that there was neither cell loss nor proliferation. Using the phenotypic criteria defined for **a–c**, the cell distribution in each population was quantified. After 5 h, only 12% of the cells were of the early phenotype, whereas >60% were of the intermediate phenotype; late cells had increased to represent >20% of the population. By 24 h, few early or intermediate cells remained and cultures consisted mainly of late cells.

ate and late cells but, in addition, a distinct peak of class II was detected in strongly anodally shifted membranes whose electrophoretic migration was identical to CIIV. Although it needs to be confirmed that these anodally shifted class II-containing membranes are functionally analogous to B-cell CIIV, it is interesting that a similar population of vesicles can be detected in developing DCs with non-lysosomal class II-containing vesicles.

To determine whether DC maturation is accompanied by altered transport of MHC class II molecules, we did pulse-chase experiments using cluster-derived early DCs or cultures containing intermediate and late cells. We first showed by metabolic labelling that the relative rates of class II synthesis were similar in the two cell populations, with late cells synthesizing ~20% more class II per hour than early cells (results not shown).

Next, early and late DCs were pulse-labelled for 20 min and the arrival of class II molecules at the plasma membrane monitored by cell-surface biotinylation^{18,19}. As shown in Fig. 3b, cell-surface delivery was strikingly inefficient in early DCs: although Ii chain-free $\alpha\beta$ dimers could be detected in total lysates within 60 min of chase, only a small fraction of these were inserted into the cell surface after 240 min (Fig. 3b, top panels). In contrast, late DCs were much better at delivering labelled class II molecules to the surface (Fig. 3b, middle panels): by 4 h, a large fraction of labelled $\alpha\beta$ dimers had reached the cell surface. This efficient delivery in late DCs was comparable to that in murine A20 cells.

The results from several pulse-chase experiments were quantified

by phosphorimaging to determine the percentage of total precipitable class II recovered after biotinylation. The results revealed that late DCs were at least 10-fold more efficient at transporting $\alpha\beta$ dimers to the surface than were early cluster-derived cells (Fig. 3c). After correcting for the inherent inefficiency of the biotinylation procedure (see Methods)¹³, we estimate that late DCs inserted at least 50% of their newly synthesized class II molecules into the plasma membrane, as compared to <5% for early cells and almost 100% for A20 B cells.

As early DCs localize most of their class II to MIIC, newly synthesized $\alpha\beta$ dimers are probably targeted to lysosomes and therefore have a different fate from those that reach the surface of late cells. In both early and late cells, peptide loading (as judged by stability in SDS) was the same (Fig. 3d), but class II molecules in early cells were degraded more rapidly than in late cells (in early cells the half-life was ~12 h, as compared to 36–40 h in late cell populations; Fig. 3e). Nevertheless, some of the class II synthesized in early cells probably did survive to reach the plasma membrane. In pulse-chase experiments done over 24 h, about 15% of the class II labelled during an initial 20 min pulse became accessible to surface biotinylation after 18 h (results not shown).

Our results are consistent with the belief that DCs accumulate antigen in the periphery and deliver it to lymphoid organs, and they indicate that peripheral early cells may sequester class II–peptide complexes intracellularly to prevent ‘premature’ presentation to T cells in the periphery. To test this, we incubated cluster-derived early

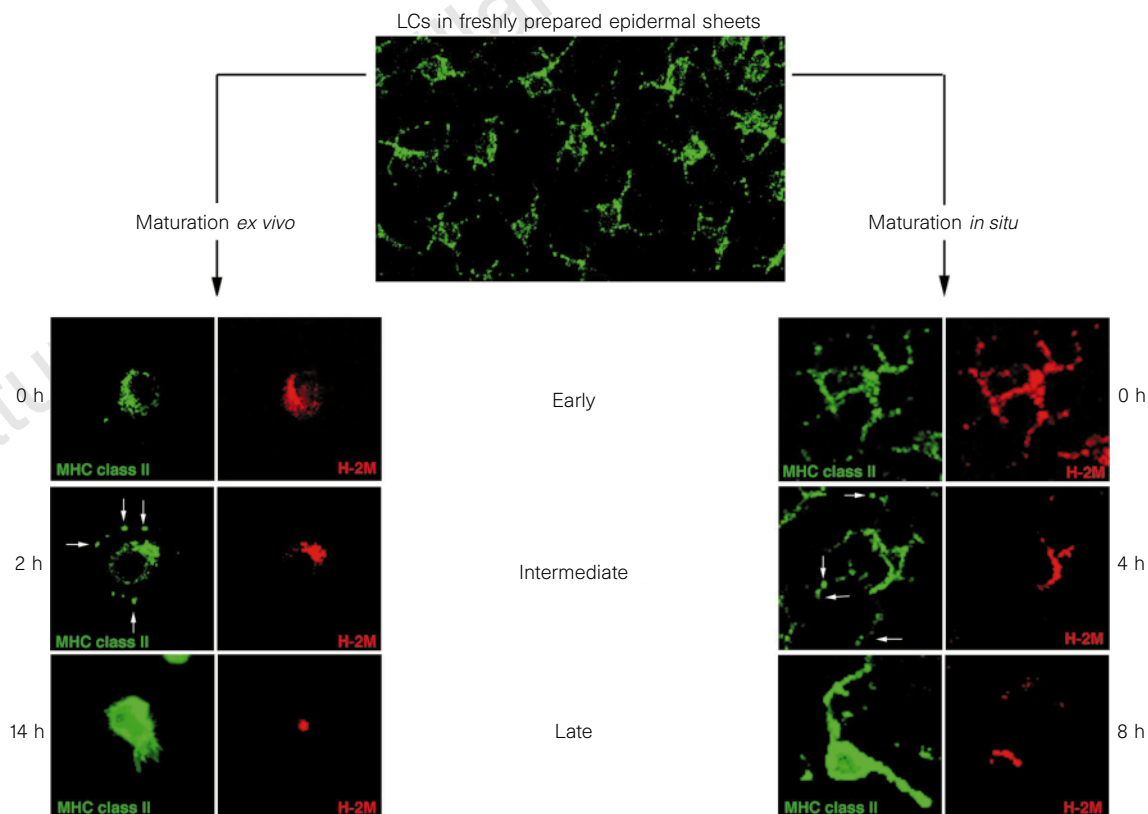


Figure 2 Developmental maturation of Langerhans cells (LCs) in culture and *in situ*. Epidermal sheets were cultured *in situ* or used for the isolation of individual LCs following collagenase treatment^{15,16}. Both explants and single cells were stained for MHC class II (using the mAb M5/114) and H2-M (using an affinity-purified rabbit antibody against the H2-M cytoplasmic domain) and visualized by confocal microscopy. Top, a low-magnification view of MHC class II-positive LCs in an intact epidermal sheet. Class II staining gives a punctate appearance in cells with typically dendritic LC morphology; cells appear to form a network throughout the epidermis. Right, higher-magnification views of LCs in epidermal sheets cultured *in situ* for 0, 4 or 8 h, and then stained for class II (green) and H2-M to mark lysosomes (red). Co-localization was strong directly after explant between class II and H2-M. Co-localization decreased with time, with H2-M staining become concentrated in the cell body while class II staining extended throughout each cell, presumably at the plasma membrane. Left, maturation of single LCs cultured for 0, 2 or 14 h *ex vivo*, that is, after isolation from an epidermal sheet. Cells were stained for class II (green) and H2-M (red) and had the morphological and organizational features of early, intermediate and late DCs from bone marrow cultures.

cells with various concentrations of ovalbumin for 3 h, washed them, and then cultured them for 0, 24 or 48 h without antigen. The cells were fixed to arrest development and assayed for immunogenic complexes. There was little presentation in the early cells fixed directly after the 3 h antigen uptake, even at very high antigen concentrations (Fig. 4). However, after incubation for 24–48 h in the absence of antigen, presentation activity increased dramatically, with virtually all of the cells achieving the mature phenotype by 48 h. Thus, immature DCs, similar to cells found in peripheral tissues, can accumulate antigen for later presentation.

A different picture emerged when the same experiment was done with the A20 B-cell line. Although widely used as an efficient antigen-presenting cell (APC), exposure of A20 cells to ovalbumin for 3 h resulted in relatively little presentation when fixed cells were assayed either before or after the chase (Fig. 4). Although our

concentrations of antigen were high, most studies with A20 cells or DCs have used 1–3-day incubations with antigen (often receptor-bound) and incubation of unfixed APCs with T cells, rather than the pulse-chase–fixation protocol used here. In control experiments, presentation was maximal for both DCs and A20 cells at >100-fold lower antigen concentrations if cells were incubated with ovalbumin for 48 h and unfixed cells were used for T-cell assays.

Early DCs in the periphery should thus accumulate antigen and newly synthesized class II molecules in lysosomes or MIIC, where processing and peptide loading can occur and the resulting immunogenic complexes can be retained. Although many of these complexes are degraded, some may survive until the DCs start maturing and class II–peptide complexes can be transferred to the plasma membrane, perhaps via the CIIV-like structures seen in the intermediate DC population. Alternatively, if only a few of the

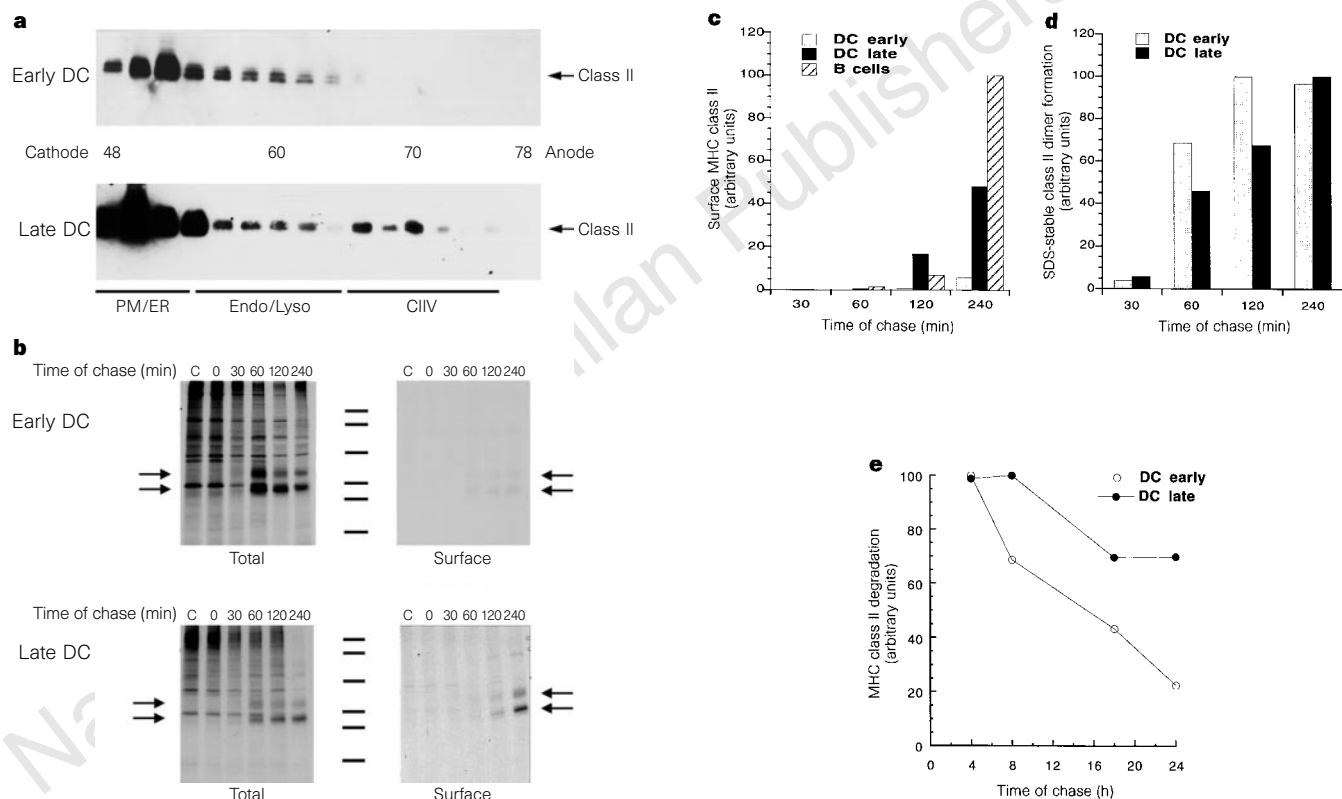


Figure 3 Intracellular transport of newly synthesized MHC class II is tightly regulated during the maturation of dendritic cells. **a**, Free-flow electrophoresis. Western blots for MHC class II β -chain corresponding to the separation by free-flow electrophoresis of intracellular membranes in early (top) or intermediate and late DCs (bottom). The separation profiles of early and late cells were virtually identical. Lysosomes (β -hexosaminidase; peak at around fraction 60) were anodally shifted relative to the plasma membrane (LFA-1; peak at around fraction 50) by at least 10 fractions (not shown). In early DCs, class II molecules were detected in the fractions corresponding to the plasma membrane (PM) (which also contained endoplasmic reticulum (ER); not shown) as well as in fractions containing endosomes and lysosomes. In intermediate and late DC populations, class II was detected in the PM/ER fractions, as well as in the endosome and lysosome fractions. A distinct peak of class II was anodally deflected relative to the major lysosome peak; this electrophoretic mobility corresponded to that of CIIV¹³. As already observed by immunofluorescence, the amount of class II present in PM-containing fractions of late DCs was much higher than for early DCs. **b, c**, Detection of class II in total cell lysates and on the cell surface. DCs and A20 B cells were pulse-labelled for 20 min and chased for the indicated times before cell-surface biotinylation. MHC class II molecules were immunoprecipitated using Y3P mAb and the surface appearance was determined by streptavidin-agarose precipitation of the biotinylated class II molecules. In total cell lysates, labelled class II became accessible to precipitation after 30 min, as expected because Y3P only detects class II molecules after $\alpha\beta$ chain dissociation²⁵. In early DCs, no class II was detected at the cell surface even after 240 min of chase. In late DCs, significant amounts of labelled class II became biotinylated at the surface after a 120-min lag, as in A20 B cells that transport nearly 100% of their class II to the surface^{13,24}. Quantification of two experiments is shown in **c**. The ratio of surface class II to total class II was corrected for biotinylation efficiency (see Methods) and expressed in arbitrary units (sample variations <20%). After 4 h, late DCs had 10-fold more class II at the surface than did early DCs, despite the fact that class II synthesis in late DCs was <20% higher than in the early cells. The total amount of class II did not change over this time, as detected by western blot. **d**, SDS-stable dimer formation was comparable in early and late DCs. Formation of SDS-stable $\alpha\beta$ dimers in early versus late DCs was determined in total cell lysates using unboiled samples for SDS-PAGE. The 65 kD SDS-stable dimer was quantified by phosphorimaging and plotted in arbitrary units. **e**, Turnover of MHC class II molecules in early and late DCs. DC cultures were labelled with ³⁵S-Translabel for 1 h and then chased for the indicated times. Total class II was immunoprecipitated using M5/114 mAb, boiled samples were analysed by SDS-PAGE, and α - or β -chain quantified by phosphorimaging. Class II half-lives were determined by linear regression to be ~12 h for early cells and 35–40 h for late cells.

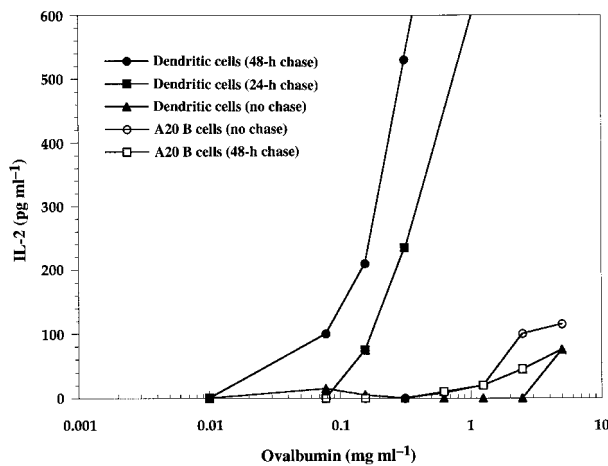


Figure 4 Early dendritic cells can accumulate antigen for presentation at a later time. Cluster-derived early DCs or A20 B cells were collected, incubated with the indicated concentrations of ovalbumin for 3 h, washed extensively, and then replated in ovalbumin-free medium for 0, 24 or 48 h before fixation and incubation with the ovalbumin-specific T-cell hybridoma DO.11. T-cell assays involved 1×10^4 DCs or 1×10^5 A20 cells incubated with 1×10^5 DO.11 cells for 24 h in 96-well plates as described²⁶. Stimulation was determined by monitoring the release of interleukin (IL)-2 by DO.11 using a solid phase enzyme-linked immunosorbent assay (ELISA) (Pharmingen). There was relatively little presentation in cells fixed directly after antigen uptake, although at the highest concentration of antigen, presentation was similar to that shown by A20 B cells. During the next 24–48 h, the presentation capacity of the DCs increased dramatically with maturation, but A20 presentation did not change significantly.

class II–peptide complexes formed in early cells survive to reach the surface, then ‘productive’ peptide loading may occur only in cells that have received a signal to initiate maturation and thus to deliver new class II molecules to the surface. These signals may be provided by cytokines or bacterial products upon the advent of infection, so antigen-presenting capacity may be coupled to inflammatory stimuli and thus the presence of foreign antigens in need of presentation. Without an inflammatory signal, DCs in the periphery should encounter only self antigens, the presentation of which by mature DCs in the periphery might break T-cell tolerance. Such a situation may be a cause of chronic inflammatory lesions²⁰.

The ability of stimulated DCs to decrease their rate of class II degradation and increase the expression of surface class II molecules is a fundamental feature of DC maturation and is also exhibited by a very different population of DCs, those derived from human peripheral blood monocytes²¹. Although ‘immature’ human monocyte-derived DCs appear to be capable of antigen presentation²¹, they may represent a later developmental stage than our bone-marrow-derived early DCs, or they may mature during T-cell assay. But both DC populations effectively retain the memory of antigens internalized earlier in development. □

Methods

Cell culture. Male BDF1 7–8-week-old mice were purchased from Charles River Laboratories (Cambridge, Massachusetts) and bone-marrow-derived DCs cultured as described⁸. Rabbit complement and monoclonal antibodies TIB120, GK1.5, TIB 211 and B220 were obtained from Pharmingen or as hybridomas (from ATCC). Recombinant murine GM-CSF was produced as a culture supernatant from J558L cells transfected with murine GM-CSF cDNA (gift from D. Gray). For some experiments, purified yeast GM-CSF (Kirin Brewing, Japan) was used, with equivalent results. Cells were washed every 2 days to remove non-adherent granulocytes and at day 6, adherent DCs, which were predominantly of the ‘early’ phenotype, were dislodged and replated in 10-cm dishes with fresh medium to generate a culture enriched in intermediate, and then in late cells by culturing for 1 and 3 days, respectively.

Cell clusters were purified by unit-gravity sedimentation on 6 ml 50% FCS columns⁸, followed by depletion for GR1-positive and/or surface class-II-positive cells by sterile cell-sorting using a Becton–Dickinson FACStar. Epidermal sheets from mouse ears were prepared as described^{15,16} and kept in RPMI 1640 supplemented with 5% FCS. Langerhans cells (LCs) were isolated by treatment of the epidermis with collagenase¹⁶ and cultivated in RPMI 1640 supplemented with 5% FCS and 1% GM-CSF.

Antibodies and immunocytochemistry. Immunofluorescence patterns were visualized by confocal microscopy as described¹². Murine I-A was detected using Rivoli affinity-purified rabbit polyclonal antibody directed against the conserved cytoplasmic tail peptide (KGPRGPPAGLLQ) of all class II I–A β -chains; H2-M was detected with ‘Ulm’ affinity-purified rabbit polyclonal antibody directed against the cytoplasmic tail peptide (KYTPLSGSTYPEGRH) of the H2-M β -chain; murine IgG-B was detected using a rat anti-mouse monoclonal antibody, GL2A7 (ref. 12). The anti-class II antibodies Y3P and M5514 antibodies are described elsewhere²² and anti LFA1/CD18 (Rb320) was a gift from P. Blier, Boehringer–Ingelheim). Anti-GR1 and Ser-4 antibodies used for immunofluorescence and FACS were obtained from Pharmingen.

Free-flow electrophoresis. 4×10^7 DCs were grown up and homogenized in 3 ml TEA buffer (10 mM triethanolamine, 1 mM EDTA, 10 mM acetic acid) with 250 mM sucrose, pH 7.4, by 10 passes in a ball-bearing homogenizer (26- μ m gap). Post-nuclear supernatants were fractionated by flotation (90 min at 37,000 r.p.m. in a Beckman SW41-Ti rotor) in a discontinuous sucrose-density gradient (1.4, 1.25, 0.25 M sucrose in TEA buffer). Low-density membranes enriched in endosomes (1.25–0.25 M interface) were collected, adjusted to 0.24 M in sucrose and briefly trypsinized (3 μ g trypsin per mg protein at 37 °C for 10 min). The reaction was stopped with an excess of soya bean trypsin inhibitor. The sample was injected into a Dr Weber GmbH Octopus PSZ free-flow electrophoresis chamber at a rate of 100 ml min⁻¹, and run at a flow rate of 250 ml h⁻¹ at 110 mA. The marker enzymes, the protein assay and details of the electrophoresis have been described^{13,23}. The distribution of MHC class II and LFA-1 was determined by western blotting of membranes collected by centrifugation (30 min at 14,000 r.p.m.).

Immunoprecipitation and cell-surface biotinylation. 3×10^7 DCs were pulse-labelled with 10 mCi in 5 ml of [³⁵S]methionine Translabel (ICN Biochemicals) in labelling medium for 20 min and chased for various times at 37 °C in RPMI/10% FCS with a 15-fold excess of cold methionine and cysteine as described^{22,24}. Radiolabelled cell pellets were lysed for 10 min on ice in 10 mM Tris, 150 mM NaCl (pH 7.4), containing 1% TX-100 (Sigma), 0.5 mM PMSF and protease-inhibitor cocktails²⁴. Lysates were pre-cleared with protein A–Sepharose (Pharmacia) at 4 °C. For surface biotinylation, intact cells were resuspended in 1 ml PBS (pH 8) and incubated with 2 mg ml⁻¹ of N-hydroxy-succinamide-S-S-biotin (HHS-SS-biotin; Pierce) for 3 min on ice as described²⁴. Lysates were immunoprecipitated overnight with Y3P anti-class II rat mAb and protein A–Sepharose. Biotinylated samples were eluted from the beads in 100 μ l PBS containing 2% SDS. 20 μ l were transferred to SDS–PAGE sample buffer (total) and the remaining 80 μ l diluted into 1 ml PBS containing 1% Empigen. Biotinylated proteins were recovered from the 80- μ l aliquot by adsorption to streptavidin–agarose beads (Pierce) for 2 h at 25 °C, which were then washed 3 times in precipitation buffer and transferred to SDS–PAGE sample buffer (surface). Immunoprecipitates were analysed on 12% gels and quantified with a Molecular Dynamics phosphorimager or by image digitization using a Visage 2000 image processor (BioImage). The efficiency of class II appearance at the plasma membrane was determined by calculating²⁴ the fraction of biotinylated class II (recovered by streptavidin–agarose) as a percentage of the total labelled class II (immunoprecipitated by Y3P from the initial cell lysate).

Received 6 June; accepted 18 June 1997.

- Steinman, R. M. The dendritic cell system and its role in immunogenicity. *Annu. Rev. Immunol.* **9**, 271–296 (1991).
- Williams, L. A., Egner, W. & Hart, D. N. Isolation and function of human dendritic cells. *Int. Rev. Cytol.* **153**, 41–103 (1994).
- Caux, C. & Banchereau, J. in *Blood Cell Biochemistry* (eds Gordon, J. & Whetton, T.) 263–301 (Plenum, London, 1996).
- Sallusto, F., Cella, M., Danieli, C. & Lanzavecchia, A. Dendritic cells use macropinocytosis and the mannose receptor to concentrate macromolecules in the major histocompatibility complex class II compartment: downregulation by cytokines and bacterial products. *J. Exp. Med.* **182**, 389–400 (1995).
- Steinman, R. M. & Swanson, J. The endocytic activity of dendritic cells. *J. Exp. Med.* **182**, 283–288 (1995).

6. Austyn, J. M. New insights into the mobilization and phagocytic activity of dendritic cells. *J. Exp. Med.* **183**, 1287–1292 (1996).
7. De Smedt, T. *et al.* Regulation of dendritic cell numbers and maturation by lipopolysaccharide *in vivo*. *J. Exp. Med.* **184**, 1413–1424 (1996).
8. Inaba, K. *et al.* Generation of large numbers of dendritic cells from mouse bone marrow cultures supplemented with granulocyte/macrophage colony-stimulating factor. *J. Exp. Med.* **176**, 1693–1702 (1992).
9. Peters, P. J., Neefjes, J. J., Oorschot, V., Ploegh, H. L. & Geuze, H. J. Segregation of MHC class II molecules from MHC class I molecules in the Golgi complex for transport to lysosomal compartments. *Nature* **349**, 669–676 (1991).
10. Kleijmeer, M. J. *et al.* MHC class II compartments and the kinetics of antigen presentation in activated mouse spleen dendritic cells. *J. Immunol.* **154**, 5715–5724 (1995).
11. Nijman, H. W. *et al.* Antigen capture and major histocompatibility class II compartments of freshly isolated and cultured human blood dendritic cells. *J. Exp. Med.* **182**, 163–174 (1995).
12. Pierre, P. *et al.* HLA-DM is expressed in conventional and unconventional MHC class II-containing compartments. *Immunity* **4**, 229–239 (1996).
13. Amigorena, S., Drake, J. R., Webster, P. & Mellman, I. Transient accumulation of new class II molecules in a novel endocytic compartment in B lymphocytes. *Nature* **369**, 113–120 (1994).
14. Jiang, W. *et al.* The receptor DEC-205 expressed by dendritic cells and thymic epithelial cells is involved in antigen processing. *Nature* **375**, 151–155 (1995).
15. Schuler, G. & Steinman, R. M. Murine epidermal Langerhans cells mature into potent immunostimulatory dendritic cells *in vitro*. *J. Exp. Med.* **161**, 526–546 (1985).
16. Larsen, C. P. *et al.* Migration and maturation of Langerhans cells in skin transplant and explants. *J. Exp. Med.* **172**, 1483–1494 (1990).
17. Marsh, M. *et al.* Rapid analytical and preparative isolation of functional endosomes by free flow electrophoresis. *J. Cell Biol.* **104**, 875–886 (1987).
18. Hunziker, W., Harter, C., Matter, K. & Mellman, I. Basolateral sorting in MDCK cells requires a distinct cytoplasmic domain determinant. *Cell* **66**, 907–920 (1991).
19. Harter, C. & Mellman, I. Transport of the lysosomal membrane glycoprotein lgp120 (lgp-A) to lysosomes does not require appearance on the plasma membrane. *J. Cell Biol.* **117**, 311–325 (1992).
20. Thomas, R. & Lipsky, P. E. Could endogenous self-peptides presented by dendritic cells initiate rheumatoid arthritis? *Immunol. Today* **17**, 559–564 (1997).
21. Cella, M., Engering, A., Pinet, V., Pieters, J. & Lanzavecchia, A. Inflammatory stimuli induce accumulation of MHC class II complexes on dendritic cells. *Nature* **388**, 782–787 (1997).
22. Germain, R. N. & Hendrix, L. H. MHC class II structure, occupancy and surface expression determined by post-endoplasmic reticulum antigen binding. *Nature* **353**, 134–139 (1991).
23. Schmid, S. L., Fuchs, R., Male, P. & Mellman, I. Two distinct subpopulations of endosomes involved in membrane recycling and transport to lysosomes. *Cell* **52**, 73–83 (1988).
24. Amigorena, S. *et al.* Invariant chain cleavage and peptide loading in post-endosomal MHC class II vesicles. *J. Exp. Med.* **181**, 1729–1741 (1995).
25. Larsen, C. P. *et al.* Regulation of immunostimulatory function and costimulatory molecule (B7-1 and B7-2) expression on murine dendritic cells. *J. Immunol.* **152**, 5208–5219 (1994).
26. Buus, S., Colon, S., Smith, C., Freed, J. H., Miles, C. & Grey, H. M. Interaction between a "processed" ovalbumin peptide and Ia molecules. *Proc. Natl Acad. Sci. USA* **83**, 3968–3971 (1986).

Acknowledgements. We thank our colleagues and R. Flavell for helpful discussions, P. Webster for electron microscopy, and P. Male for confocal microscopy. P.P. was supported by a long-term EMBO fellowship, S.J.T. by an NIH predoctoral training grant, and R.M.S. and I.M. by NIH research grants.

Correspondence and requests for materials should be addressed to I.M. (e-mail: ira.mellman@yale.edu).

Distinct actions of *cis* and *trans* ATP within the double ring of the chaperonin GroEL

Hays S. Rye[†], Steven G. Burston[†], Wayne A. Fenton[†], Joseph M. Beechem[‡], Zhaohui Xu[§], Paul B. Sigler^{*§} & Arthur L. Horwich^{*†}

^{*}Howard Hughes Medical Institute, [†]Department of Genetics, School of Medicine, and [§]Department of Molecular Biophysics and Biochemistry, Yale University, New Haven, Connecticut 06510, USA

[‡]Department of Molecular Physiology and Biophysics, Vanderbilt University, Nashville, Tennessee 37232, USA

The chaperonin GroEL is a double-ring structure with a central cavity in each ring that provides an environment for the efficient folding of proteins^{1–3} when capped by the co-chaperone GroES in the presence of adenine nucleotides^{4–8}. Productive folding of the substrate rhodanese has been observed in *cis* ternary complexes, where GroES and polypeptide are bound to the same ring, formed with either ATP, ADP or non-hydrolysable ATP analogues^{2,9}, suggesting that the specific requirement for ATP is confined to an action in the *trans* ring that evicts GroES and polypeptide from the *cis* side⁹. We show here, however, that for the folding of malate dehydrogenase and Rubisco there is also an absolute requirement for ATP in the *cis* ring, as ADP and AMP-PNP are unable to

promote folding. We investigated the specific roles of binding and hydrolysis of ATP in the *cis* and *trans* rings using mutant forms of GroEL that bind ATP but are defective in its hydrolysis. Binding of ATP and GroES in *cis* initiated productive folding inside a highly stable GroEL–ATP–GroES complex. To discharge GroES and polypeptide, ATP hydrolysis in the *cis* ring was required to form a GroEL–ADP–GroES complex with decreased stability, priming the *cis* complex for release by ATP binding (without hydrolysis) in the *trans* ring. These observations offer an explanation of why GroEL functions as a double-ring complex.

The monomeric protein rhodanese has recently been shown to reach native form inside *cis* ternary GroEL–GroES complexes that were formed in ATP, AMP-PNP or ADP, albeit at different rates (ATP > AMP-PNP > ADP)^{2,9}. The single-ring GroEL mutant SR1 has been used to produce obligate and stable *cis* complexes for study^{1,2,9}. Because it has no second ring, the SR1 mutant does not receive the signal from *trans*-sided ATP that normally evicts GroES and substrate⁶. After GroES and any of the three nucleotides were added to rhodanese–SR1 binary complexes, productive folding was shown to occur in the *cis* cavity. We observed that rhodanese that was refolded inside SR1–GroES formed in the presence of ATP could be released efficiently to the medium by brief incubation at 4 °C, a treatment previously shown to lead to rapid dissociation of GroES from an ADP complex with GroEL⁶. Similarly, folding of ornithine transcarbamylase (OTC) from binary complexes with SR1 occurred in the presence of GroES, with almost identical kinetics with either ATP or ADP, when GroES was released by incubation at 4 °C, thereby allowing OTC trimerization (data not shown). These data suggest that the previous observation of OTC folding in the presence of ATP in a single turnover from a *cis* ternary complex¹ resulted from ADP-driven folding during preparation of the complex, with subsequent release when ATP was added. In experiments using SR1 and the green fluorescent protein (GFP), which also refolds inside *cis* complexes formed with any of the three nucleotides, brief treatment at 4 °C also leads to efficient release of GFP (Fig. 1a).

When the same tests were performed with two stringent substrate proteins, Rubisco from *Rhodospirillum rubrum*^{10,11} and mitochondrial malate dehydrogenase (MDH) from pig heart^{12–14}, we observed that only ATP could promote reactivation from wild-type or SR1 *cis* ternary complexes (Fig. 1b, c). Release of GroES from SR1 by treatment at 4 °C was essential for production of enzymatic activity, because both Rubisco and MDH are homodimers, requiring assembly of the refolded monomeric subunits to reach active form. Direct incubation at 4 °C of metastable intermediates of Rubisco that were produced after dilution from denaturant (into the same chloride-free buffer used in all of the Rubisco studies)⁶ did not result in enzymatic activity (data not shown). Remarkably, the kinetics of reactivation by the SR1–GroES ternary complexes in ATP were similar to, if not faster than, those achieved in similar reactions with wild-type GroEL, indicating that a stable folding-active state is produced at SR1. Addition of 'trap' molecules (such as 337/349)¹⁵, which are able to bind but not release non-native substrate proteins, at the time of cold release of GroES had no effect on the kinetics of reactivation (kinetics not shown, but see Fig. 1f, traces 1, 4). These data indicate that, as with rhodanese, folding of both Rubisco and MDH proceeded to a committed state in the ATP *cis* ternary complexes; that is, the substrates reached conformations no longer recognizable by chaperonin.

We wished to follow directly the folding of substrate within the various *cis* complexes, thereby obviating any requirement for the release of GroES and peptide to assay enzymatic activity. We therefore examined by stopped-flow changes in the fluorescence total intensity and anisotropy of tryptophan residues of Rubisco in complexes formed following the addition of GroES and nucleotides to Rubisco–chaperonin binary complexes (Fig. 1d, e). This takes advantage of the absence of tryptophan from both GroEL and